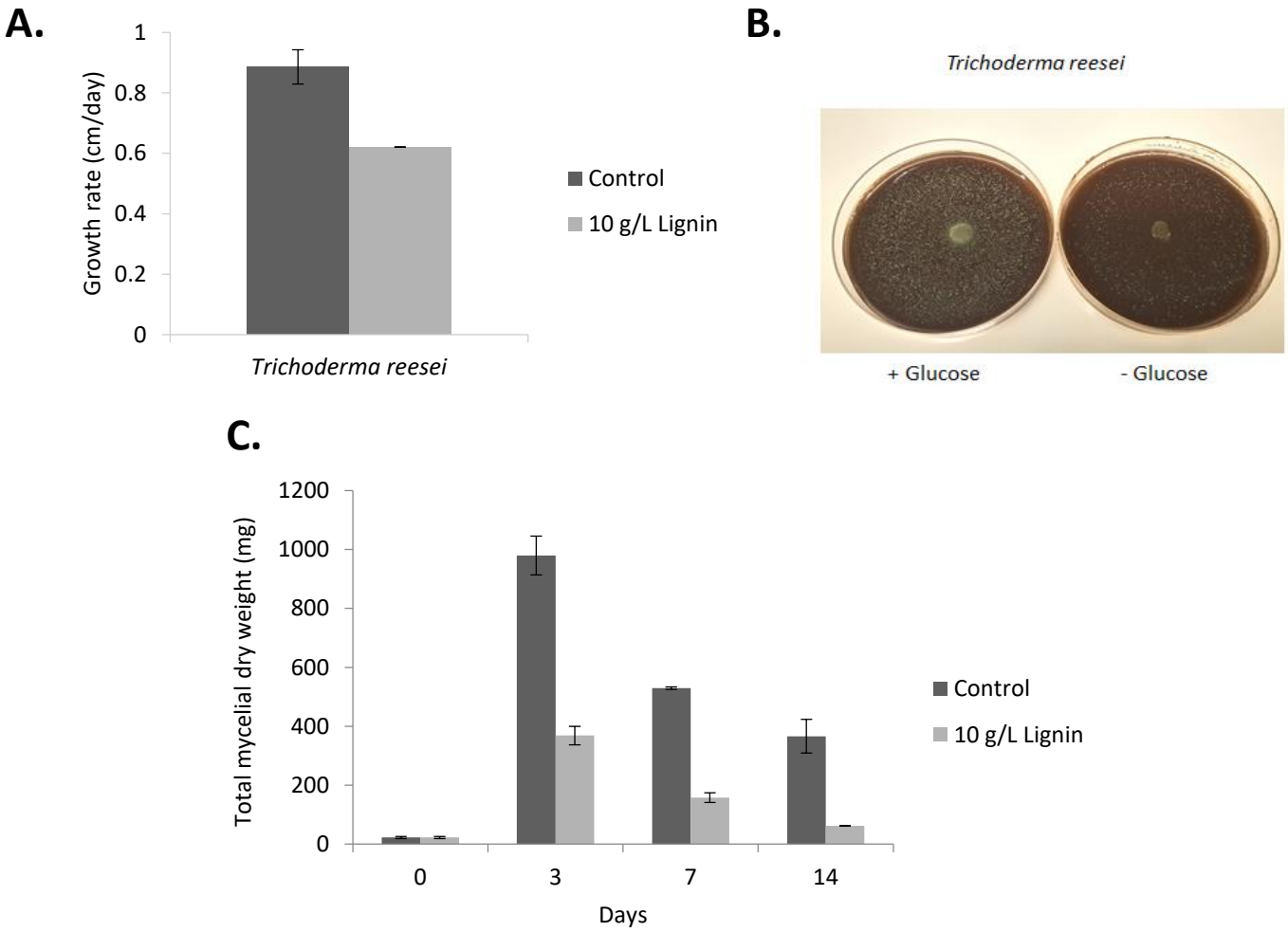

Figure S1. *T. reesei* growth on technical soda lignin. A. Growth rate of *T. reesei* on agar plates containing technical lignin in the presence and absence of 1 g/L glucose and **B.** mycelial appearance. **C**. Total mycelial dry weight of *T. reesei* during growth in liquid cultures on lignin in the presence and absence of 2.5 g/L maltose.

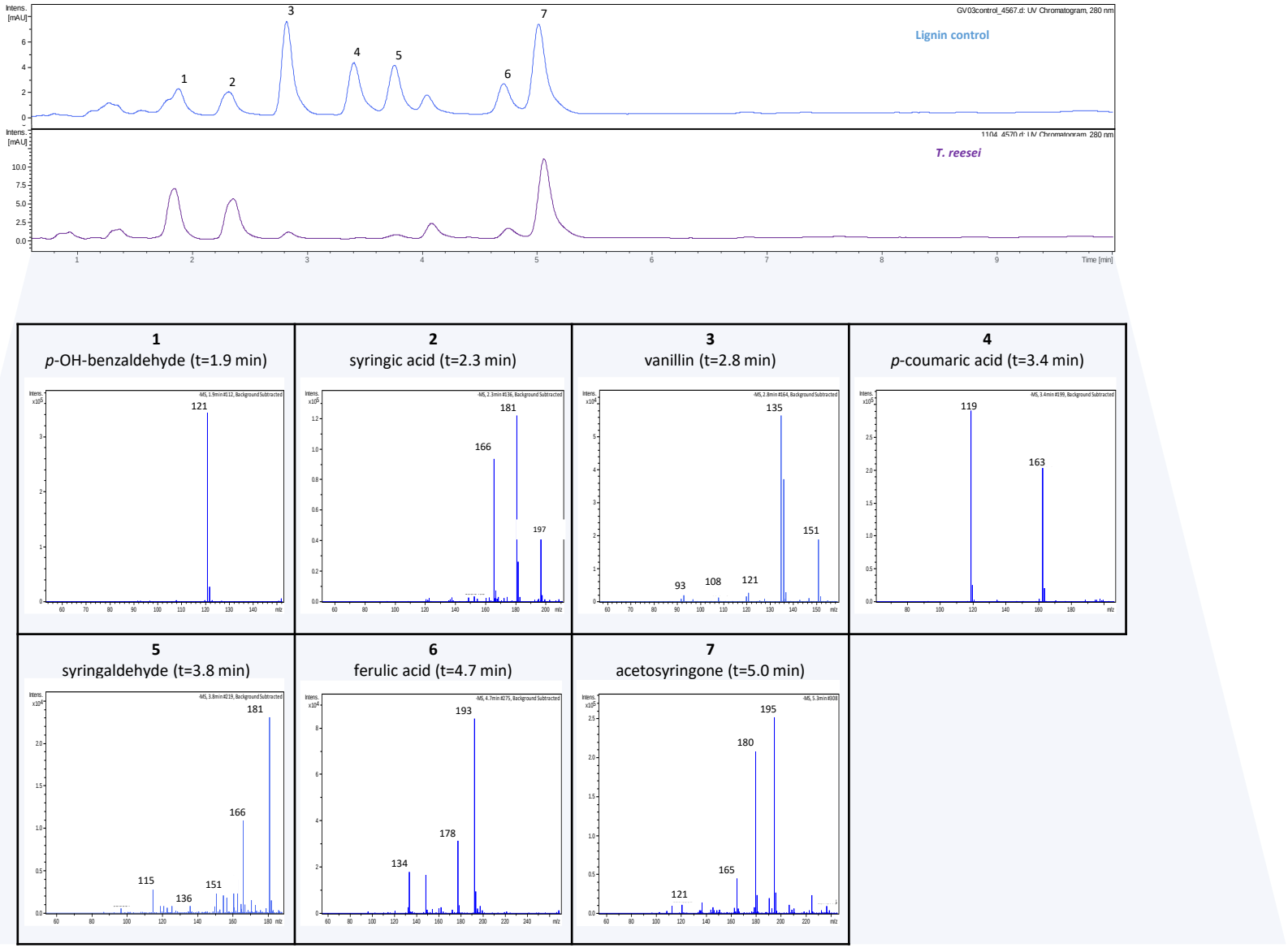

Figure S2. LC-MS analysis on water-soluble lignin fraction. The analysis is done on phenolic monomers extracted from the culture supernatant by ethyl acetate. Normalized chromatograms obtained with a C18 column (Highpurity, Thermo Electron Corporation, 2.7 µm, 50 mm x 2 mm I.D.mm), a 5–100 vol.% aqueous acetonitrile, 1‰ HCOOH gradient (30min) and 0.4 ml/min flow rate, and with a 280 nm UV detection. ESI-MS spectra were obtained in the negative mode from scans acquired in a mass range of m/z 120–2000.

Table S1. **Total phenolic and thioacidolysis yields of water-insoluble residual lignin after exposure to *T. reesei.***

	PheOH (mmol g^{-1})[a]	**Thioacidolysis[b]**	
		Total yield (µmol g^{-1})	**S/G ratio**
Control	2.90	132 ± 9	0.93 ± 0.05
T. reesei	2.80	89 ± 3	0.92 ± 0.00

[a] Data correspond to single determination

[b] Data are mean values (± standard error) between duplicate analyses.

Table S2. Identified CAZymes in the secretomes during growth of *T. reesei* on technical lignin.

Protein ID	Cazy	Day of growth	Protein ID	Cazy	Day of growth
22915	AA3_2	7	69276	GH30_7	7 and 14
80659	AA3_3	14	82235	GH31	3, 7 and 14
124282	**AA5_1**	**3, 7 and 14**	80240	GH35	3, 7 and 14
78357	AA6	7 and 14	124016	GH36	3, 7 and 14
73643*	AA9-CBM1	7	123226	GH37	3, 7 and 14
77299	GH2	3, 7 and 14	3196	GH38	14
69245	GH2	3, 7 and 14	68064	GH43	7
62166*	GH2	7	45717	GH47	3, 7 and 14
58450	GH3	3, 7 and 14	55319	GH54-CBM42	3, 7 and 14
121735	GH3	3, 7 and 14	123283	GH54-CBM42	3, 7 and 14
121127	GH3	3, 7 and 14	121746	GH55	3, 7 and 14
47268	GH3	7	54242	GH55	3, 7 and 14
76672	GH3	7 and 14	70845	GH55	3, 7 and 14
104797	GH3	7 and 14	73248	GH55	3, 7 and 14
82616*	GH5_5	7	76210	GH62	3, 7 and 14
120312	CBM1-GH5_5	7	124175	GH64	3, 7 and 14
56996	GH5_7	7	123456	GH65-CBM32	3, 7 and 14
72567	CBM1-GH6	7 and 14	72526	GH67	3, 7 and 14
123989	GH7-CBM1	3, 7 and 14	71532	GH71	3, 7 and 14
122081	GH7-CBM1	7 and 14	108672	GH71-CBM24-CBM24	3, 7 and 14
120229*	GH10	7	120873	GH71-CBM24-CBM24	3, 7 and 14
74223	GH11	7 and 14	123538*	GH72	7
123818	GH11	3, 7 and 14	22914	GH72-CBM43	3, 7 and 14
123232*	GH12	7	82633	GH72-CBM43	3, 7 and 14
105956	GH13_1	3, 7 and 14	49081	GH74-CBM1	3, 7 and 14
1885	GH15-CBM20	3, 7 and 14	70341*	GH75	7
65406	GH16	3, 7 and 14	74807*	GH76	7 and 14
123726	GH16	3, 7 and 14	27395	GH76	7
49274	GH16	3, 7 and 14	67844*	GH76	7
39755	GH16	7	106575	GH79	3, 7 and 14
76266*	CBM18-GH16	7	71394	GH79	7
66792	GH17	3, 7 and 14	57098	GH92	3, 7 and 14
39942	GH17	3, 7 and 14	55733	GH92	3, 7 and 14
80833	GH18	3, 7 and 14	60635	GH92	7 and 14
119859	GH18	7 and 14	79921*	GH92	7
68347	GH18-CBM1	7 and 14	58802	GH95	3, 7 and 14
21725	GH20	3, 7 and 14	111138*	GH95	7
23346	GH20	7	5807*	GH95	7
103458	GH25	7	79606	GH115	7 and 14
72632	GH27	3, 7 and 14	70373	GH125	7 and 14
59391	GH27	3, 7 and 14	107850	CE1	7
27259*	GH27	7	44214	CE5	3, 7 and 14
122780	GH28	3, 7 and 14	73632*	CE5-CBM1	3 and 7
103049	GH28	7 and 14	58282	CE9	14
3094	GH30_3	3, 7 and 14	121418	CE16	3, 7 and 14
69736	GH30_3	7 and 14	103033	PL7_4	7
110894	GH30_5	3, 7 and 14	69189*	PL20	7
111849	GH30_7	3, 7 and 14			

*proteins that were exclusively detected in the absence of maltose.

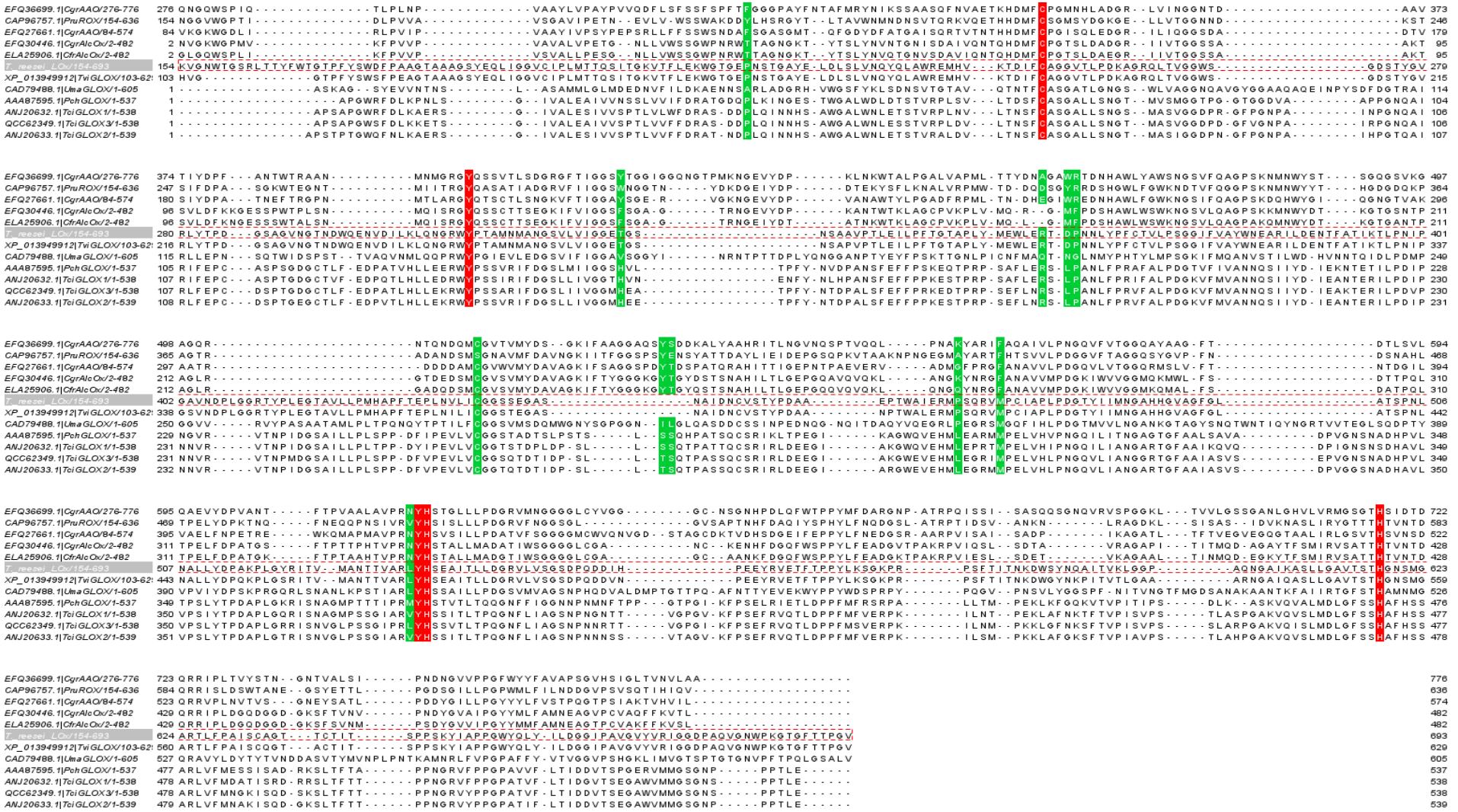

Figure S3. Sequence alignment of 11 functionally characterized AA5 enzymes with *Tr*LOx. EFQ36699.1: aryl alcohol oxidase from *Colletotrichum graminicola*; CAP96757: Raffinose oxidase from *Penicillium rubens*; EFQ27661: aryl alcohol oxidase from *C. graminicola*; EFQ30446: Alcohol oxidase from *C. graminicola*; ELA25906: Alcohol oxidase from *C. fructicola*; XP_013949912: Glyoxal oxidase from *T. virens*; CAD79488: Glyoxal oxidase from *Ustilago maydis*; AAA87595: Glyoxal oxidase from *Phanerochaete chrysosporium*; ANJ20632: Glyoxal oxidase 1 from *Trametes cinnabarina*; QCC62349: Glyoxal oxidase 3 from *T. cinnabarina*; ANJ20633: Glyoxal oxidase 1 from *T. cinnabarina.* Residues involved in copper binding are highlighted in red and other residues involved in enzymatic activity and substrate preference are highlighted in green.

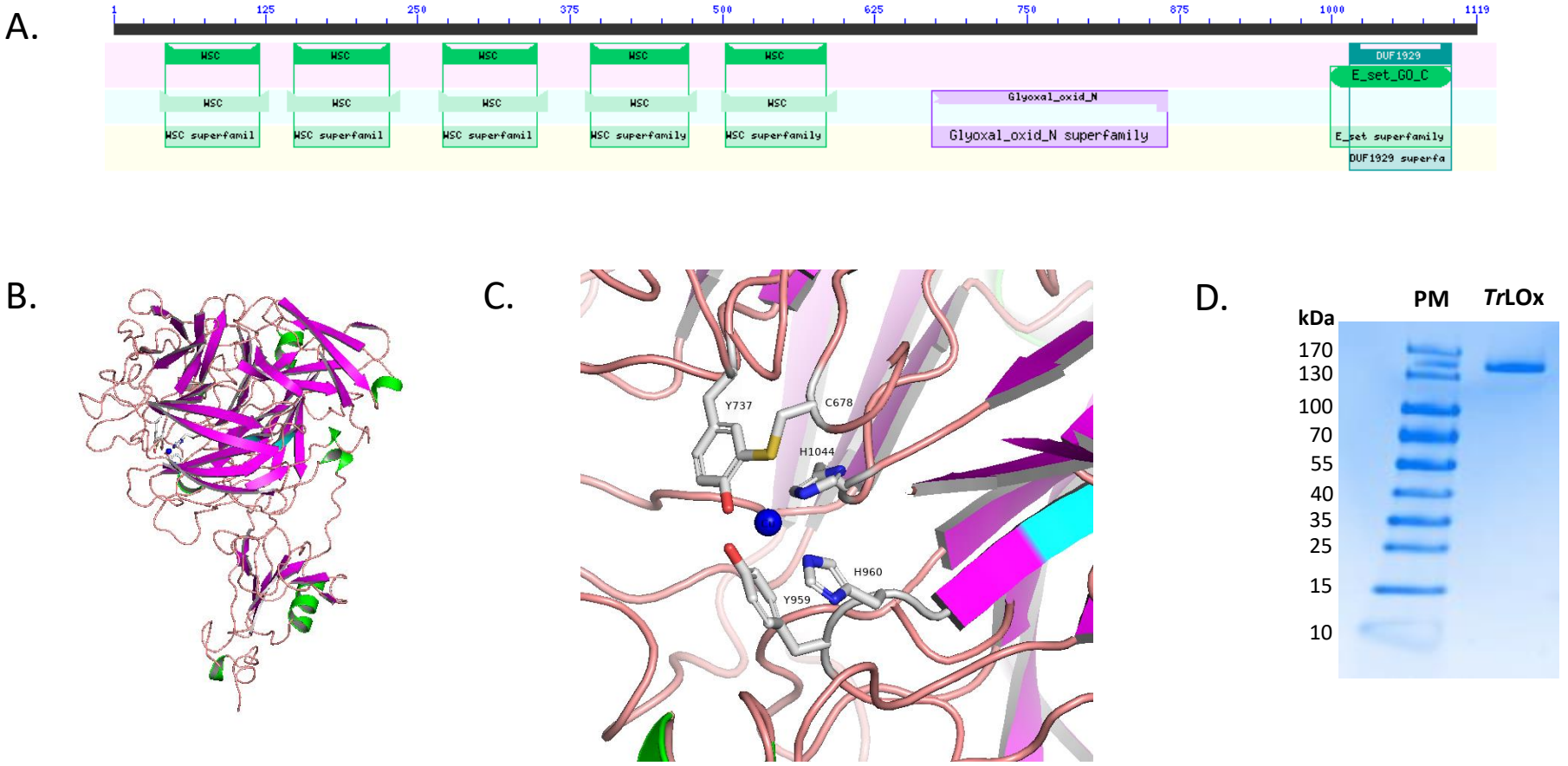

Figure S4. Structural characteristics of *Tr*LOx. A. Predicted domain and functional sites in *Tr*LOx encoding sequence. WSC domain: wall stress-responsive component; E_set_GO_C: C-terminal Early set domain associated with the catalytic domain of galactose oxidase at the C-terminal end; DUF1929: Domain of unknown function. **B.** Predicted molecular structure of *Tr*LOx. The model was generated using Phyre2 and with copper oxidase from *Colletotrichum graminicola* as template (PDB 6RYX). **C.** The active site of *Tr*LOx containing the aromatic residues implicated in copper coordination. **D.** SDS-PAGE gel of purified *Tr*LOx protein.

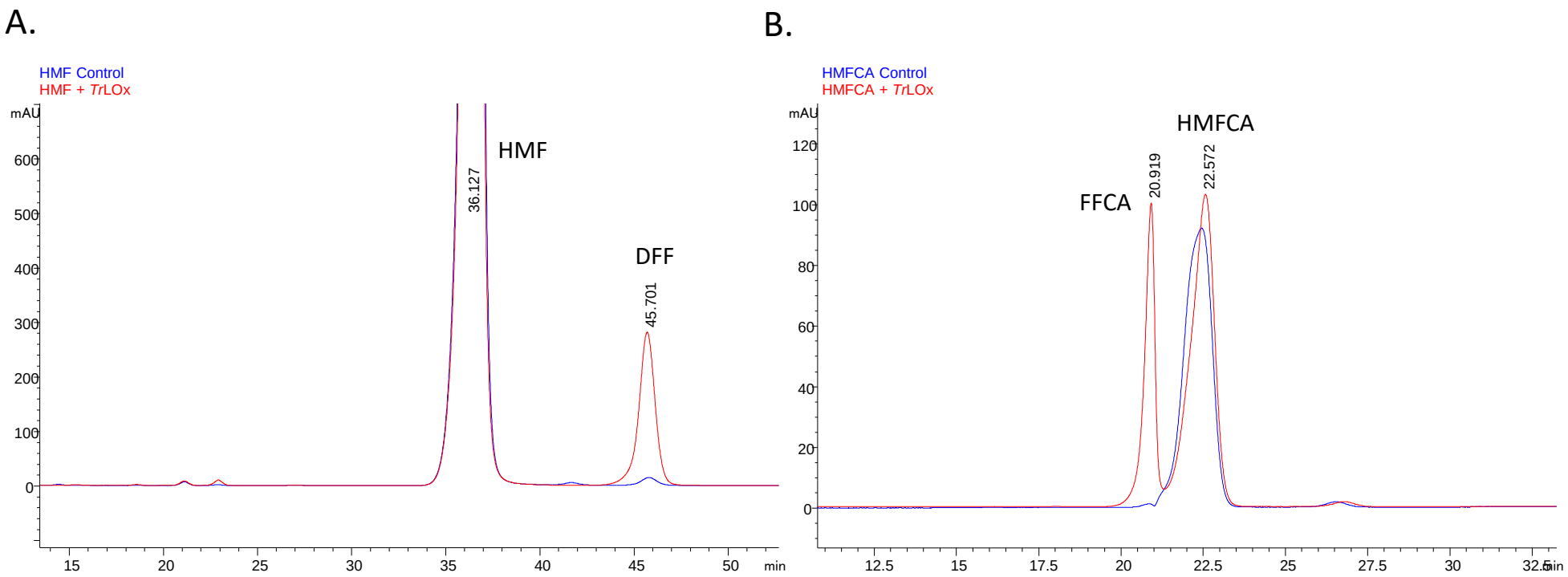

Figure S5. HPLC analysis of *Tr*LOx reactions on A. HMF and B. HMFCA. The reactions were performed at 30 °C under agitation at 800 rpm over 24 h period in 50 mM tartrate buffer pH 6 and in the presence of 10 µg of enzyme and 5 mM of substrate. Reaction mixtures were separated on Aminex HPX87H column (300 × 7.8 mm) (BioRad) at 45 °C, with 2.5 mM sulfuric acid as the isocratic mobile phase with a flow rate of 0.6 mL/min. Eluted compounds were detected using a diode array detector at 280 nm. The reactions were stopped by incubating the mixture at 90 °C for 10 min and centrifuging at 15,000×g for 15 min. In blue are HMF and HMFCA standards and in red is the reaction with *Tr*LOx.

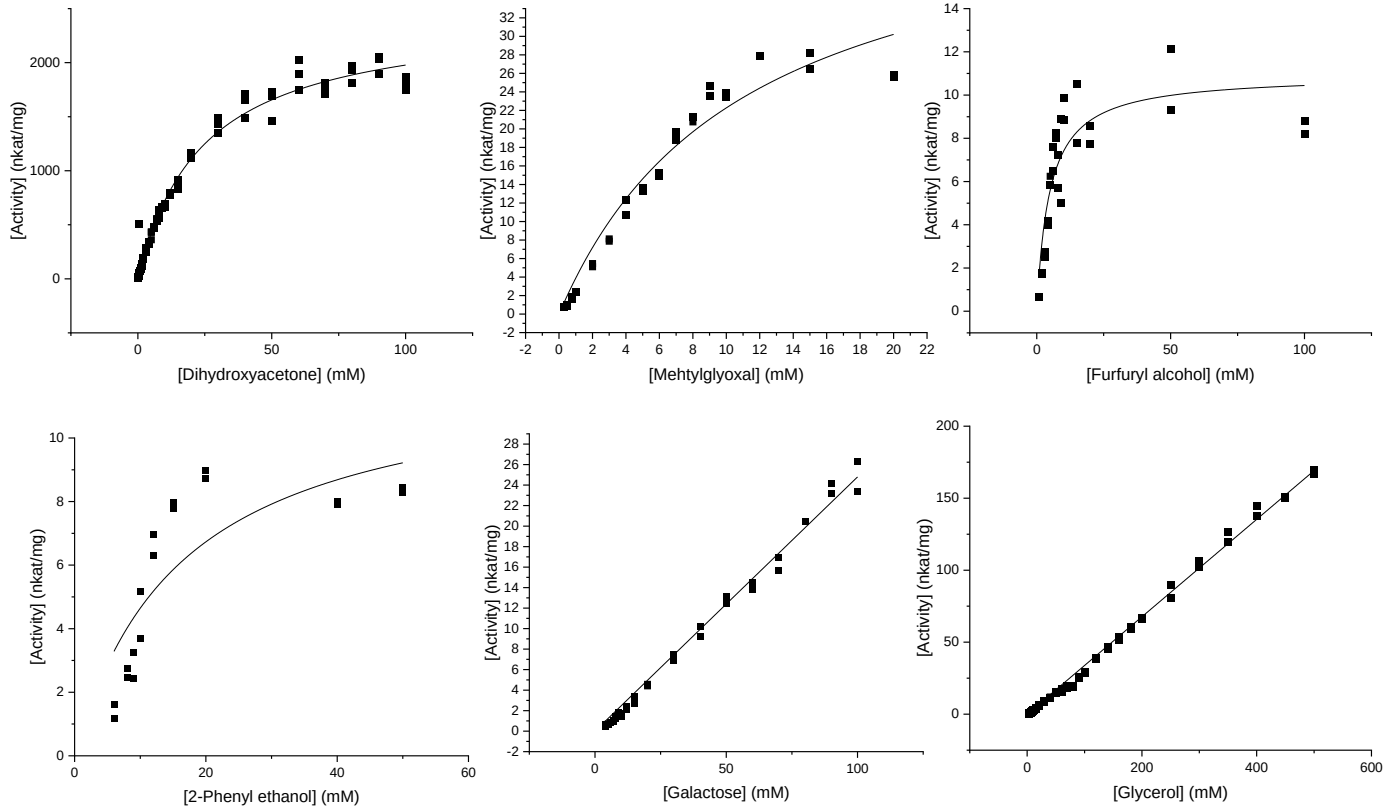

Figure S6. Michaelis–Menten plots for the activity of *Tr*LOx on the different tested substrates.

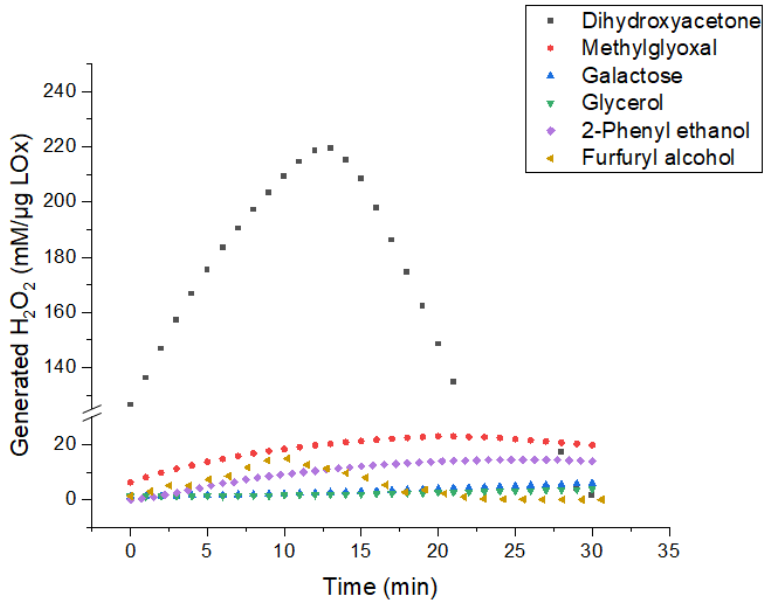

Figure S7. H_2O_2 production overtime in the reaction of *Tr*LOx on different substrates. The fluorescence was followed at an excitation wavelength of 560 nm and an emission wavelength of 595 nm. The slope from the standard curve relating H_2O_2 concentration and fluorescence was used to calculate the amount of generated H_2O_2 over time (0-20 µM H_2O_2; 374.34 counts/µmol).

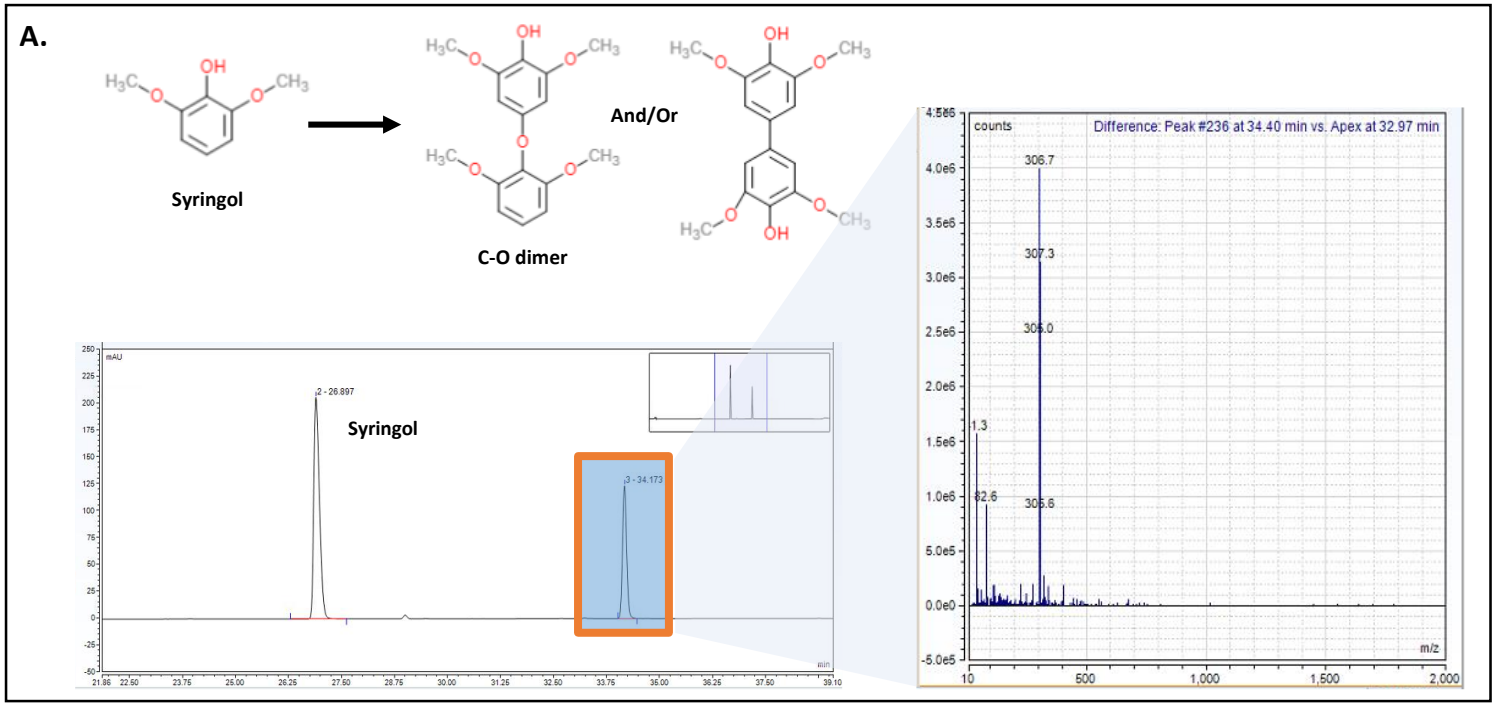

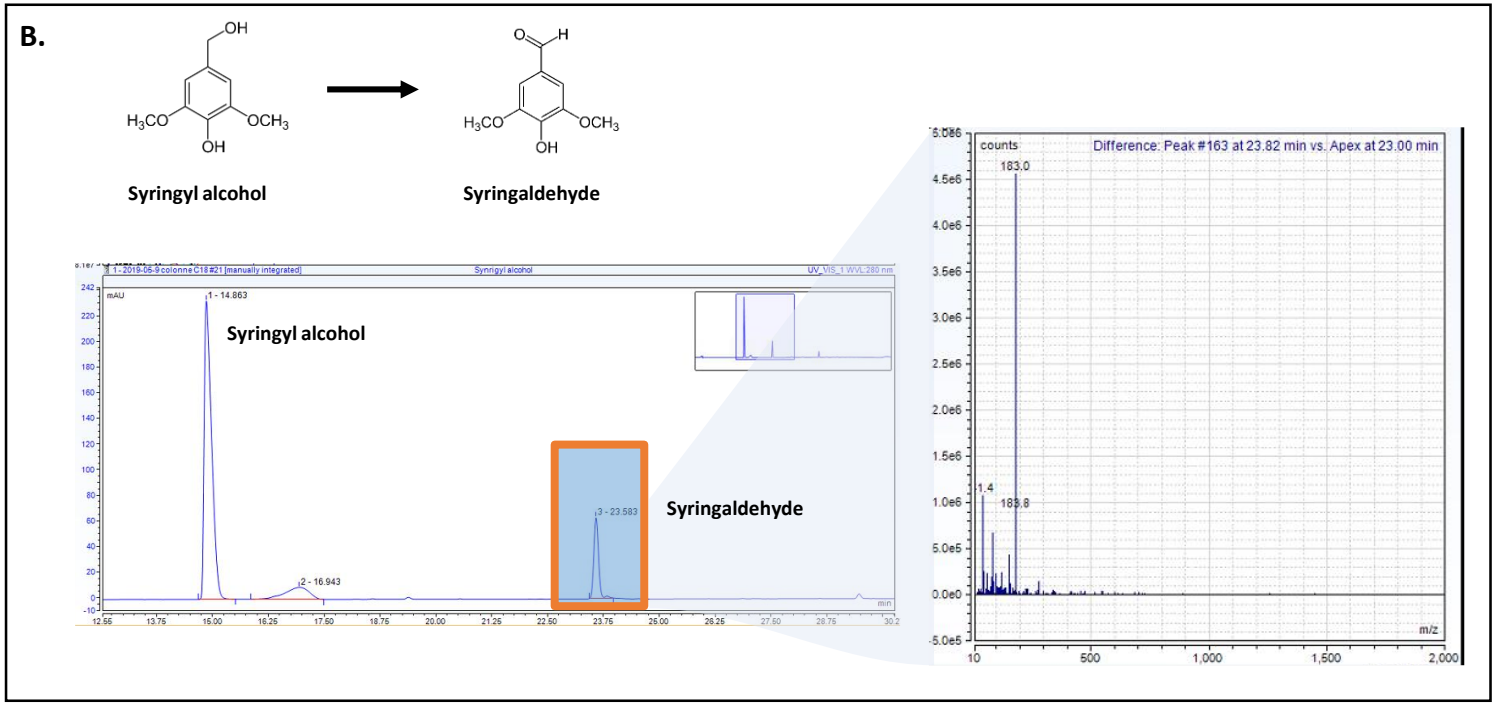

Figure S8. LC-MS chromatograms of the reaction of *Tr*LOx on A. Syringol and B. Syringyl alcohol. The molecular weight of the detected product with syringol (306.7) suggest the formation of C-C and/or C-O dimers.